JBC RESEARCH ARTICLE

Hypoxia-inducible factor-1α and poly [ADP ribose] polymerase 1 cooperatively regulate Notch3 expression under hypoxia *via* a noncanonical mechanism

Received for publication, September 29, 2021, and in revised form, May 5, 2022 Published, Papers in Press, June 14, 2022,
https://doi.org/10.1016/j.jbc.2022.102137

Hideaki Nakamura[1,2,*], **Hiroki Sekine**[3], **Hiroyuki Kato**[4], **Hisao Masai**[5], **Katarina Gradin**[1], **and Lorenz Poellinger**[1,4,†]

From the [1]*Cell and Molecular Biology, Karolinska Institutet, Stockholm, Sweden;* [2]*Department of Transfusion Medicine, Saga University Hospital, Saga, Japan;* [3]*Department of Gene Expression Regulation, Institute of Development, Aging and Cancer, Tohoku University, Sendai, Japan;* [4]*Cancer Science Institute of Singapore, National University of Singapore, Singapore, Republic of Singapore;* [5]*Genome Dynamics Project, Department of Basic Medical Sciences, Tokyo Metropolitan Institute of Medical Science, Setagaya, Tokyo, Japan*

Edited by Dennis Voelker

Upregulation of *Notch3* expression has been reported in many cancers and is considered a marker for poor prognosis. Hypoxia is a driving factor of the Notch3 signaling pathway; however, the induction mechanism and role of hypoxia-inducible factor-1α (HIF-1α) in the Notch3 response are still unclear. In this study, we found that HIF-1α and poly [ADP-ribose] polymerase 1 (PARP-1) regulate Notch3 induction under hypoxia *via* a noncanonical mechanism. In the analyzed cancer cell lines, *Notch3* expression was increased during hypoxia at both the mRNA and protein levels. HIF-1α knockdown and *Notch3* promoter reporter analyses indicated that the induction of Notch3 by hypoxia requires HIF-1α and also another molecule that binds the *Notch3* promoter's guanine-rich region, which lacks the canonical hypoxia response element. Therefore, using mass spectrometry analysis to identify the binding proteins of the *Notch3* promoter, we found that PARP-1 specifically binds to the *Notch3* promoter. Interestingly, analyses of the *Notch3* promoter reporter and knockdown of PARP-1 revealed that PARP-1 plays an important role in Notch3 regulation. Furthermore, we demonstrate that PARP inhibitors, including an inhibitor specific for PARP-1, attenuated the induction of Notch3 by hypoxia. These results uncover a novel mechanism in which HIF-1α associates with PARP-1 on the *Notch3* promoter in a hypoxia response element–independent manner, thereby inducing Notch3 expression during hypoxia. Further studies on this mechanism could facilitate a better understanding of the broader functions of HIF-1α, the roles of Notch3 in cancer formation, and the insights into novel therapeutic strategies.

Notch is a transmembrane cell surface receptor that plays crucial roles in a variety of cellular processes and is related to various diseases (1, 2). In mammals, four Notch receptors (Notch1-4) and five ligands are components of the Notch signaling pathway. The binding of the ligand to the Notch receptor induces cleavage of the receptor, and subsequently, γ-secretase additionally cleaves the truncated receptor and leads to the release of the Notch intracellular domain. Finally, Notch intracellular domain translocates to the nucleus and forms a complex with the transcriptional regulator RBPJ (also called CSL or CBF1) to induce target gene expression. All Notch receptors share a similar structure, but Notch3 and Notch4 have a shorter intracellular domain than Notch1 and Notch2 and lack the transactivation domain (3, 4). A large number of studies have shown numerous physiological roles of Notch1 and Notch2, but little is known about Notch3 and Notch4. Recent reports have shown that high expression of Notch3 is correlated with poor prognosis in various types of cancers. Notch3 activation is highly involved in apoptosis, invasion, metastasis, and resistance to chemotherapy (5–10). Thus, the development of therapies targeting Notch3 is in progress (11, 12). Interestingly, several reports indicate that Notch3 is induced by hypoxia, but the precise mechanism of Notch3 upregulation remains unclear (13–15).

Hypoxia is a microenvironmental feature of many solid cancers, which arises from an imbalance between cellular O_2 consumption and supply. Hypoxia is recognized as a key factor linked to aggressive cancer phenotypes and resistance to chemotherapeutic agents and irradiation therapies (16–18). Hypoxia-inducible factor-1α (HIF-1α) is a well-established transcriptional activator that mediates responses to hypoxia-related physiological changes. HIF-1α forms a dimer with HIF-1β, and the heterodimer translocates to the nucleus to activate the expression of target genes by binding to a conserved motif (A/GCGTG) in the gene promoter called the hypoxia response element (HRE). This HRE-dependent activation manner by hypoxia-inducible factor (HIF) is recognized as a canonical mechanism. Induction of target genes by HIF has been linked to several biological pathways and allows cancer cells to adapt to hypoxia, resulting in the acquisition of malignant phenotypes and resistance to therapies (19–21). To date, reports on HIF target genes are increasing every year (22). In contrast to the canonical mechanism of transcriptional

† Deceased.
* For correspondence: Hideaki Nakamura, sr3977@cc.saga-u.ac.jp.

activation by HIF, HRE-independent activation mechanisms have rarely been reported (23–25).

Poly [ADP-ribose] polymerases (PARPs) are a family of enzymes that can modify proteins by ADP-ribosylation (26). The best-studied member, PARP-1, has been shown to be a key regulator of DNA damage and genomic maintenance (27, 28). Currently, PARP inhibitors have been increasingly approved for clinical use, mainly for cancers with DNA-repair deficiencies (29, 30). Interestingly, PARP-1 regulates gene transcription through several mechanisms, such as DNA methylation, chromatin regulation, histone modification, and transcription factor binding (31–34). A comprehensive analysis has shown that PARP-1 positively regulated gene transcription (35). The interaction of PARP-1 with NF-κB or E2F-1 increases the expression of the target gene *CXCL1* or *MYC*, respectively (36, 37). PARP-1 also interacts with HIF-1α, and the complexes can activate HIF-1α target gene expression (38–40). Interestingly, the loss of *Parp-1* affects *Notch3* expression, although the precise mechanism remains unclear (35).

In our study, we have focused on analyzing the molecular mechanisms of *Notch3* regulation under hypoxia and demonstrated that HIF-1α and PARP-1 cooperatively increased Notch3 expression under hypoxic conditions. The association of HIF-1α and PARP-1 with a non-HRE sequence in the *Notch3* promoter is indispensable for this regulation, which is distinct from the canonical HIF-1α transcriptional activation mechanism. These findings should contribute to further elucidation of this newly discovered unique molecular function of HIF-1α and the role of Notch3 in cancer.

Results

Notch3 expression at both mRNA and protein levels is increased under hypoxia

We first examined *Notch3* expression during hypoxia in HeLa and SK-N-BE(2)c cell lines. These cells were cultured under normoxia or hypoxia for 4 or 24 h, and total RNA was evaluated by reverse transcription-quantitative PCR (RT-qPCR). Significant induction of *Notch3* mRNA was observed when we cultured the cells at 1% hypoxia for 24 h in accordance with well-known hypoxia-induced genes, such as *PGK1* and *CA9* (Fig. 1*A*). Then, we examined the protein levels of Notch3 in HeLa, SK-N-BE(2)c, and SK-N-FI cells by immunoblotting. Expression of full-length Notch3 was upregulated in HeLa and SK-N-BE(2)c cells, under hypoxia (Fig. 1*B*). Expression of the Notch3 intracellular domain (N3ICD), which is functionally more relevant, was elevated in all cell lines.

Next, we examined the effects of HIF-1α on hypoxia-induced Notch3 using siRNA against *HIF1A*. One of two siHIF1As or a nonspecific siRNA (siNS) was transiently transfected into SK-N-BE(2)c cells, and the cells were cultured under normoxia or hypoxia for 24 h. Thereafter, we performed RT-qPCR analysis using total RNA from the cultured cells. Both siHIF1As significantly decreased *HIF1A* expression in normoxia and hypoxia, and in the siHIF1A-transfected cells, induction of *Notch3* by hypoxia was attenuated as compared to siNS. In particular, siHIF1A-2 strongly inhibited *Notch3* induction by hypoxia. The induction of *PGK1* and *CA9* by hypoxia was also attenuated in siHIF1A-transfected cells (Fig. 1*C*). Interestingly, the levels of N3ICD and full-length Notch3 under hypoxia were decreased by siHIF1A treatment (Fig. 1*D*). Consistent with mRNA analysis, siHIF1As, especially siHIF1A-2, showed significant inhibition of Notch3 protein expression under hypoxia. These data strongly indicate that HIF-1α plays a role in the induction of Notch3 by hypoxia.

Promoter activities of Notch3 are induced by hypoxia or HIF-1α

To clarify the mechanism of the induction of *Notch3* by hypoxia, we subcloned the 5′ region of the human *Notch3* (from −188 to +77) into a luciferase reporter plasmid, pGL4.10 vector, and performed reporter analysis. The reporters were transiently transfected into HeLa cells, and the cells were cultured under normoxia or hypoxia for 24 h prior to luciferase reporter analysis. As a result, pGL4.10-*Notch3* pro −188 bp had a much higher promoter activity than the empty plasmid vector pGL4.10 under normoxia. As expected, *Notch3* promoter activity was upregulated under hypoxia, suggesting that the promoter region contained a hypoxic response region (Fig. 2*A*). To determine the region responsible for this induction, we constructed shorter *Notch3* promoter reporters (*Notch3* promoter −57 to +77 or −10 to +77) and performed a luciferase assay. The results indicated that the hypoxia response region resides in the *Notch3* promoter from −57 to −10 bp (Fig. 2*A*).

To elucidate the effects of HIF-1α on *Notch3* promoter activity, we performed cotransfection analysis using the *Notch3* promoter reporters and HIF-1α expression plasmid (2–826). As a result, HIF-1α enhanced the reporter activities of *Notch3* (Fig. 2*B*, lower panel). Since the promoter region is highly guanine-rich and has no canonical HRE sequence, the HIF-1α domain required for *Notch3* promoter activation was next examined. For this purpose, we constructed a set of HIF-1α deletion mutants (Fig. 2*B* upper panel) and performed cotransfection assays. These results indicate that HIF-1α transactivating domains (HIF-1α 530–826) alone can increase *Notch3* promoter activity, and the N-terminal DNA binding domain is dispensable for this activity.

HIF-1α physically associates with the Notch3 promoter

To further analyze the binding of HIF-1α to the *Notch3* promoter, we performed a pull-down analysis using biotinylated *Notch3* promoter oligonucleotide and streptavidin-sepharose. HeLa cells were cultured under normoxic or hypoxic conditions for 24 h, and nuclear extracts were prepared. The biotinylated oligos were incubated with nuclear extracts before incubation with streptavidin-sepharose. The bound proteins were eluted and analyzed by immunoblotting. HIF-1α was strongly detected in the biotinylated *Notch3* promoter oligo mixed with nuclear extracts from cells cultured under hypoxia, but not under normoxia (Fig. 3*A* above image, lane 6). We next added nonbiotinylated *Notch3* promoter oligos or nonbiotinylated control oligos together with the biotinylated oligos and the nuclear extracts in a competition assay. As

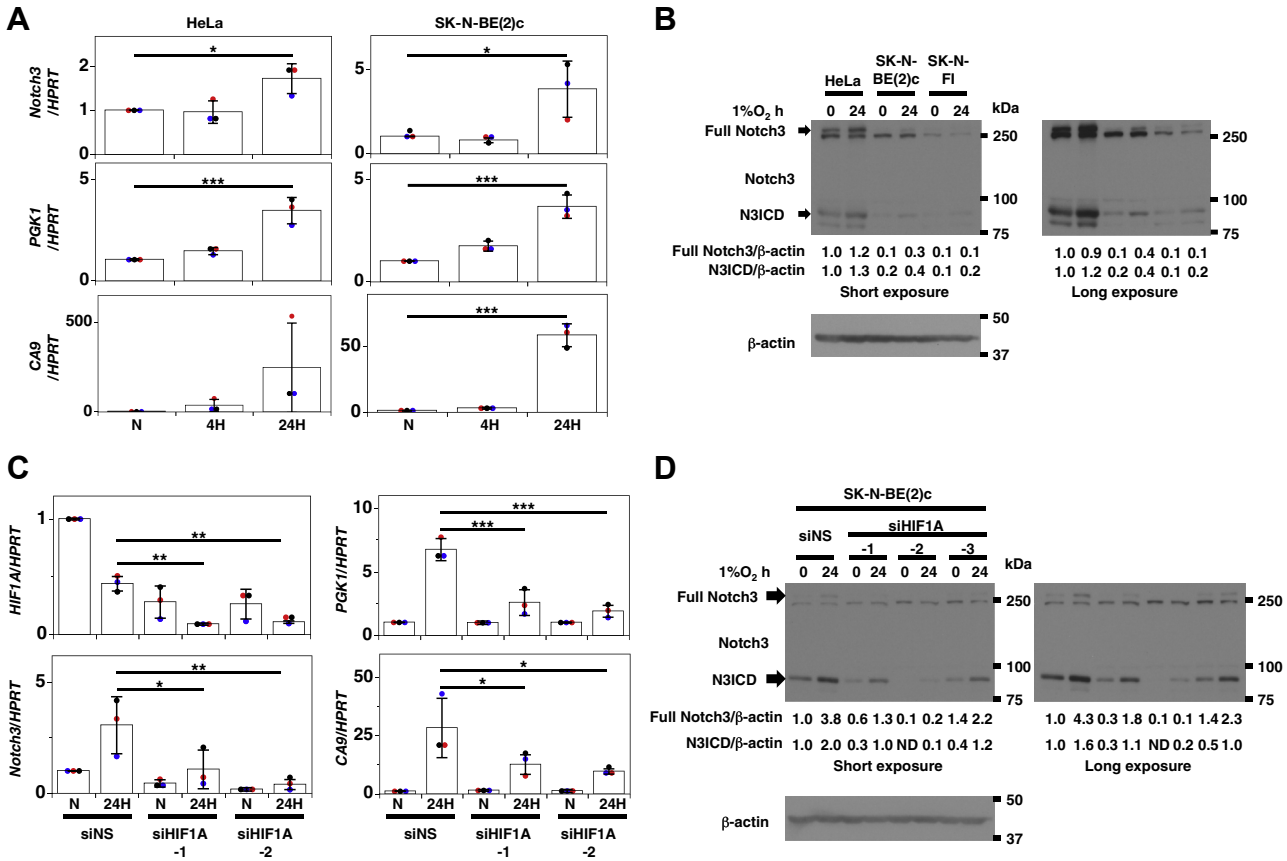

Figure 1. Hypoxia increases *Notch3* expression depending on HIF-1α in cancer cell lines. *A*, HeLa and SK-N-BE(2)c cells were incubated under normoxia or an indicated period of hypoxia. Expression levels of *Notch3*, *PGK1*, and *CA9* mRNA were analyzed by RT-qPCR. Relative mRNA levels were calculated as the ratio to that of *HPRT*. *Dots* with each color represent means of triplicates. The overall mean values and SD calculated from the three different experiments (*black*, *red*, and *blue*) were shown as a bar graph with an error bar. *B*, HeLa, SK-N-BE(2)c, and SK-N-FI cells were cultured under normoxia or hypoxia for 24 h. Protein levels of Notch3 and β-actin were evaluated by immunoblotting. Images by short and long exposures were shown. Arrows indicate the full-length Notch3 (Full Notch3) and the Notch3 intracellular domain (N3ICD) bands. Values by quantification after normalized to HeLa cells in 1% O_2 for 0 h are presented under the lanes. The band density of Full Notch3 was low, therefore the values were semiquantitative or qualitative. *C* and *D*, *HIF1A* knockdown assays were performed in SK-N-BE(2)c cells. SK-N-BE(2)c cells were transfected with targeted siRNA for *HIF1A* (siHIF1A) or control siRNA (siNS) and cultured under normoxic or hypoxic conditions for 24 h. *C*, expression levels of *HIF1A*, *Notch3*, *PGK1*, and *CA9* were analyzed by RT-qPCR. Relative mRNA levels were analyzed as in (*A*). *D*, protein levels of Notch3 and β-actin were analyzed as in *B*. Values by quantification after normalized to siNS in 1% O_2 for 0 h are presented under the lanes. The Tukey-Kramer HSD test was used as a post hoc test for comparisons between the indicated groups in (A) and (C). $*p < 0.05$; $**p < 0.01$; $***p < 0.001$. Full Notch3, full-length Notch3; HIF-1α, hypoxia-inducible factor-1α; N3ICD, Notch3 intracellular domain; RT-qPCR, reverse transcription-quantitative PCR; siNS, nonspecific siRNA.

expected, HIF-1α levels were evidently attenuated by adding the nonbiotinylated *Notch3* promoter oligo compared to lane 6 (Fig. 3*A* above image, lane 7). On the other hand, the addition of the nonbiotinylated control oligo (Fig. 3*A* above image, lane 8) slightly decreased the HIF-1α level. This suggests that HIF-1α can bind to the *Notch3* promoter region with no apparent HRE and likely activates *Nocth3*. Thus, our results raised the hypothesis that HIF-1α binds to the *Notch3* promoter sequence in cooperation with other proteins.

PARP-1 binds to the Notch3 promoter and increases the promoter activity

To identify proteins that bind to the *Notch3* promoter, we performed a mass spectrometry analysis. Proteins bound to the *Notch3* promoter oligo were analyzed by SDS-PAGE and visualized by silver staining. Remarkable bands were observed near 110 kDa in lanes 3 to 6 (Fig. 3*B*). The band in lane 5, which was challenged with the nonbiotinylated *Notch3* promoter oligo, was significantly weaker than that in the other lanes. The resolved gel was stained with CBB G-250, and the excised bands were analyzed by mass spectrometry (Fig. S1). The 110 kDa band was unequivocally identified as PARP-1 (Table S3). To clarify PARP-1 binding to the *Notch3* promoter, we verified it with an antibody against PARP-1 using the samples used to detect HIF-1α. PARP-1 was observed in both normoxia and hypoxia samples (Fig. 3*A* lower image, lanes 5 and 6), and the level was preferentially decreased by adding the nonbiotinylated *Notch3* promoter oligo compared to lane 6 (Fig. 3*A* lower image, lane 7). Although little is known about the relationship between PARP-1 and Notch3, the physical interaction between PARP-1 and HIF-1α has been reported (38–40). To validate this interaction in our experimental system, we performed a pull-down assay using extracts from HeLa cells stably expressing FLAG-tagged HIF-1α (F-HIF-1α). F-HIF-1α was induced by a prolyl-hydroxylase inhibitor $CoCl_2$ (Fig. S2*A*), meaning that the band (F-HIF-1α) is subject to the hypoxia-induced degradation control. By the

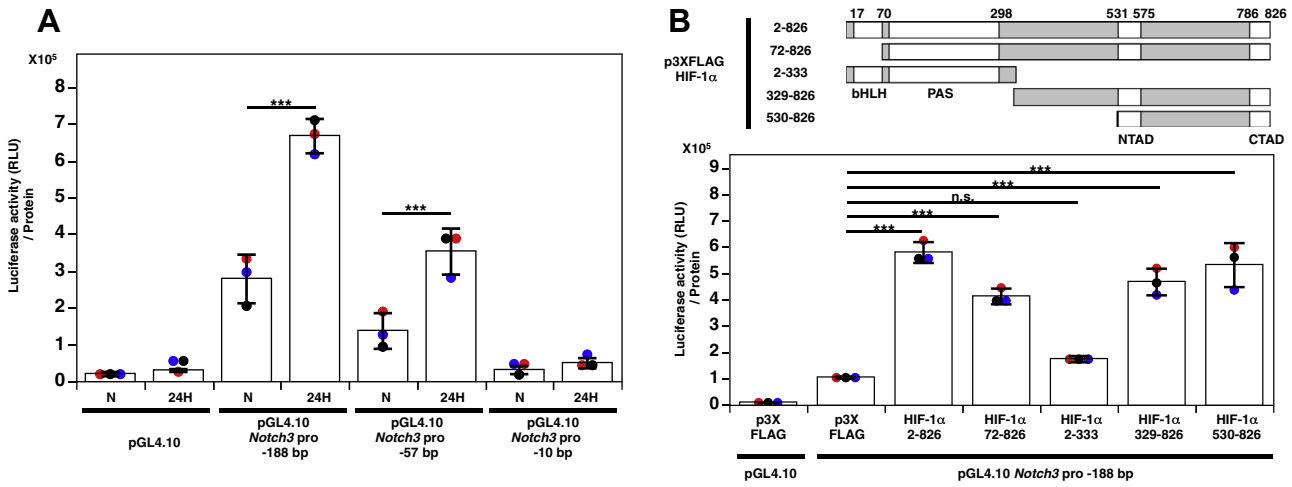

Figure 2. HIF-1α increases *Notch3* promoter activities *via* a noncanonical mechanism. *A*, luciferase reporter plasmids containing the *Notch3* promoter region (−188, −57, or −10 to +77) were used. Each reporter plasmid was transfected into HeLa cells and incubated for 24 h under normoxia (N) or hypoxia (24 h). Thereafter, luciferase reporter activities were determined. Reporter activities were measured with normalization by protein concentration. Luciferase analysis was performed three times each with triplicate. The individual mean values calculated from the three technical samples were shown in different colored dot plots (*black*, *red*, and *blue*). The overall mean values and SD were then calculated and presented. The Tukey-Kramer HSD test was used as a post hoc test for comparisons between the indicated groups. *B*, the upper panel indicates a schematic representation of HIF-1α expression plasmids in the cotransfection reporter assay. The lower panel shows that each reporter and HIF-1α expression plasmids were cotransfected into HeLa cells, and promoter reporter activities were evaluated as in (*A*). Dunnett's test by comparing with the group of p3XFLAG was used as a post hoc test. ***$p < 0.001$; n.s., not significant. HIF-1α, hypoxia-inducible factor-1α.

pull-down *via* F-HIF-1α, endogenous PARP-1 was significantly detected (Fig. S2*B*), suggesting that HIF-1α interacts with PARP-1 even without the target DNA sequence. Since HIF-1α was pulled down with PARP-1 by the *Notch3* promoter oligo (Fig. 3), we presumed that HIF-1α binding to the *Notch3* promoter was dependent on PARP-1. To test this, a pull-down assay with purified PARP-1 and HIF-1α (Fig. S2*C*) by the combination was conducted. PARP-1 was successfully precipitated by the oligo, and remarkably, both the full-length HIF-1α and the C-terminal region (530–826) of HIF-1α (HIF-

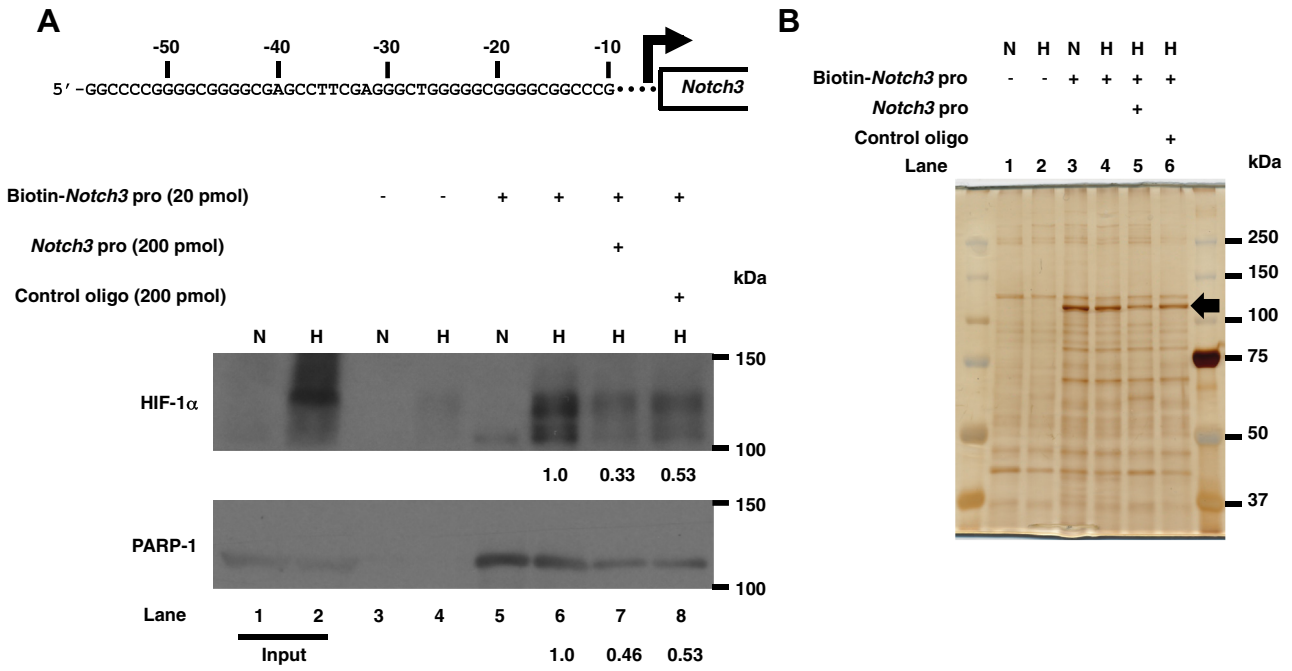

Figure 3. HIF-1α and PARP-1 bind to the *Notch3* promoter. *A*, pull-down assay by the *Notch3* promoter oligonucleotide. Upper panel shows the *Notch3* promoter sequence (−57 to −10 bp from the transcription start site). Lower panel indicates the following. HeLa cells were cultured under normoxia or hypoxia for 24 h, and nuclear extracts were prepared. Initially, biotinylated oligos (Biotin-*Notch3* pro) were combined with the nuclear extracts, and streptavidin-sepharose was added to the complex. Thereafter, binding proteins were eluted and the HIF-1α and PARP-1 levels were analyzed by immunoblotting. Nonbiotinylated oligo (*Notch3* pro) or control oligo were used for competition analysis. Values by quantification after normalized to lane 6 are presented under the lanes. *B*, pulled down proteins by the biotinylated oligo were analyzed by SDS-PAGE. Protein bands in the gel were visualized by silver staining. The specific and prominent 110 kDa band indicated by the *arrow* was excised for identification by mass spectrometry. HIF-1α, hypoxia-inducible factor-1α; PARP-1, poly [ADP-ribose] polymerase 1.

1α C) were efficiently coprecipitated with PARP-1 (Fig. S2*D*). This clearly indicates that the C-terminal region of HIF-1α interacts with the *Notch3* promoter sequence *via* PARP-1.

We analyzed the functional effects of PARP-1 on *Notch3* expression using a luciferase reporter assay. We constructed a series of the following PARP-1 expression plasmids: full-length PARP-1 (2–1014), N-terminal PARP-1 (2–533), or C-terminal PARP-1 (531–1014) (Fig. 4*A*, upper panel). The *Notch3* promoter reporter and the PARP-1 expression plasmid were cotransfected into HeLa cells and the cells were incubated for 24 h. Luciferase reporter assay showed that the full length of PARP-1 increased the *Notch3* promoter from −57 to +77 bp reporter activity compared to the control (p3XFLAG), whereas no remarkable changes were seen in the *Notch3* promoter −10 to +77 bp reporter. The results suggested that PARP-1 acted on the *Notch3* promoter −57 to −10 region, and thus this region was used for binding analysis. Furthermore, induction of *Notch3* reporter activity by the N-terminal or C-terminal part of PARP-1 was significantly lower than by the full length of PARP-1 (Fig. 4*A*, lower panel). These data indicate that PARP-1 plays a crucial role in the induction of *Notch3*, and both the N-terminal and C-terminal domains of PARP-1 are required for the induction.

PARP-1 induces Notch3 under hypoxia and the induction is reduced by PARP inhibitors

We performed PARP-1 knockdown analysis using RNAi. SK-N-BE(2)c cells were transiently transfected with one of two siRNAs targeting RARP-1 (siPARP-1s) or siNS, cultured under normoxia or hypoxia for 24 h, and analyzed by RT-qPCR. No remarkable changes in *PARP-1* expression under hypoxia compared to normoxia were observed. However, the expression of *PARP-1* was significantly decreased by siPARP-1s (Fig. 4*B*), whereas no remarkable effect was observed on *HIF1A* (Fig. S3*A*). The attenuation of *Notch3* induction under hypoxia by *PARP-1* knockdown was statistically significant (Fig. 4*B*). Little or no remarkable difference was observed in the expression of the representative HIF targets *PGK1* and *CA9* (Fig. 4*B*), suggesting that PARP-1 does not directly act on HRE-containing promoters. We next analyzed the effects of siPARP-1s on the expression of the Notch targets *HEY1* and

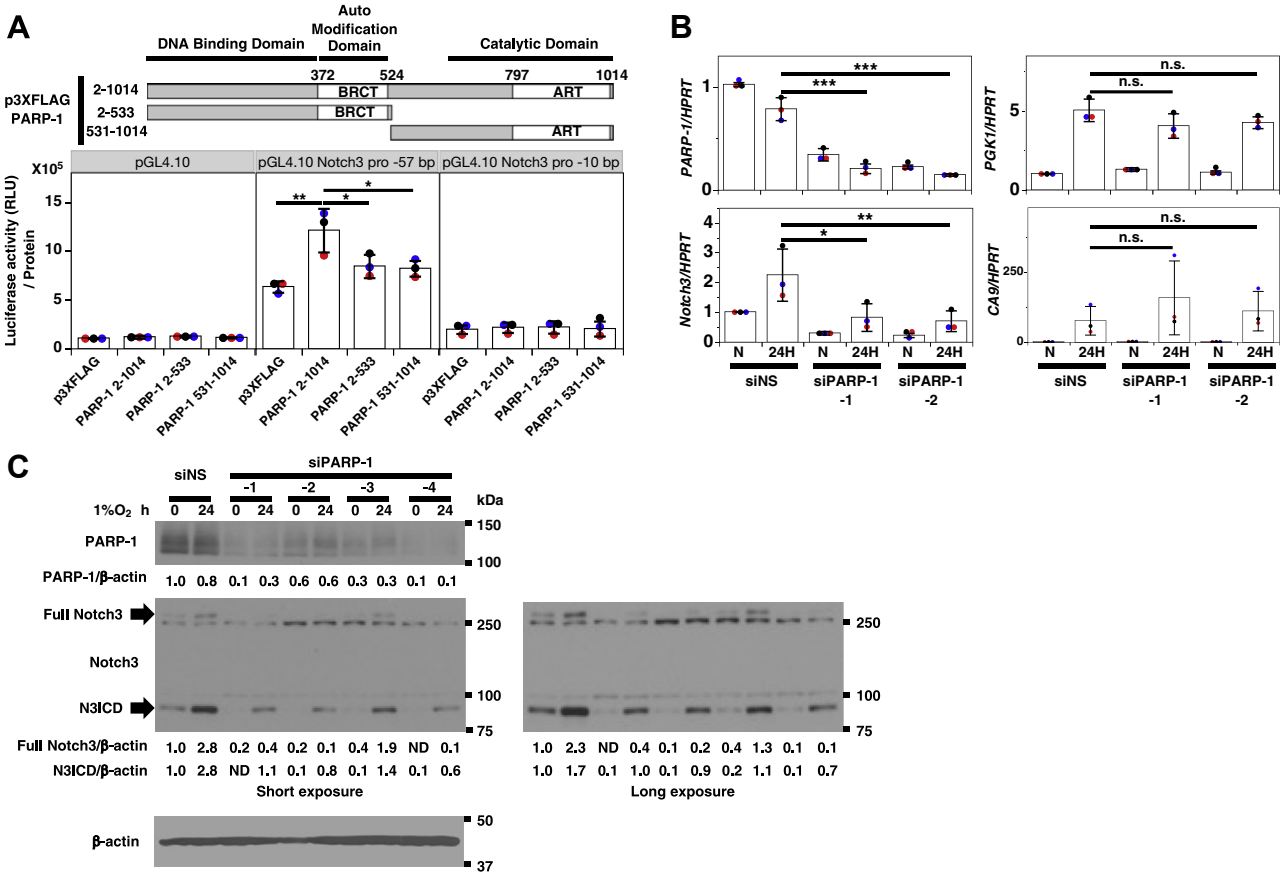

Figure 4. PARP-1 activates *Notch3* expression by acting on the *Notch3* promoter. *A*, upper panel indicates a schematic representation of PARP-1 expression plasmids that were used in the cotransfection reporter assay. Lower panel shows that each reporter and PARP-1 expression plasmids were cotransfected into HeLa cells, and promoter reporter activities were evaluated as Figure 2*A*. Dunnett's test by comparing with the group of full-length PARP-1 was used as a post hoc test. *$p < 0.05$; **$p < 0.01$. *B* and *C*, *PARP-1* knockdown assays were performed in SK-N-BE(2)c cells. Targeted siRNA for *PARP-1* (siPARP-1) or control siRNA (siNS) was transfected into the cells and cultured under normoxic or hypoxic conditions for 24 h. *B*, expression levels of *PARP-1*, *Notch3*, *PGK1*, and *CA9* were analyzed in the transfected SK-N-BE(2)c cells by RT-qPCR. Relative mRNA levels were calculated as the ratio to that of *HPRT*. The statistical analysis was performed and shown in the same way as Figure 1*A*. *$p < 0.05$; **$p < 0.01$; ***$p < 0.001$. *C*, protein levels of PARP-1, Notch3, and β-actin were evaluated in the cell lines by immunoblotting. *Arrows* indicate Full Notch3 and N3ICD bands. Values by quantification after normalized to siNS in 1% O_2 for 0 h are presented under the lanes. Full Notch3, full-length Notch3; N3ICD, Notch3 intracellular domain; n.s., not significant; PARP-1, poly [ADP-ribose] polymerase 1; RT-qPCR, reverse transcription-quantitative PCR; siPARP-1s, siRNAs targeting RARP-1; siNS, nonspecific siRNA.

HES1. Mostly, siPARP-1s significantly downregulated *HEY1* and *HES1* preferentially under hypoxia (Fig. S3*A*). We also performed immunoblotting, and the protein levels of PARP-1 were significantly reduced by siPARP-1s. Similar to changes in the mRNA levels, Notch3 but not HIF-1α at the protein level was remarkably decreased in PARP-1 knockdown cells (compare Fig. 4*C* with Fig. S3*B*). These data indicated that PARP-1 plays a key role in the regulation of *Notch3* expression. Next, we analyzed the effects of PARP inhibitors. We used BYK204165 (BYK), a selective inhibitor of PARP-1, and PJ-34, a PARP inhibitor (41). SK-N-BE(2)c cells were treated with DMSO, BYK, or PJ-34, cultured under normoxic or hypoxic conditions for 24 h, and analyzed by RT-qPCR. Expression of *Notch3*, but not *PARP-1*, under hypoxia, was attenuated by both inhibitors. BYK had a much stronger inhibitory effect on *Notch3* expression under hypoxia than on PJ-34 (Fig. 5*A*). We also analyzed these inhibitors' effects on the expression of *PGK1* and *CA9*. The hypoxic induction of *PGK1* and *CA9* was significantly decreased by BYK, albeit milder than that of *Notch3* (Fig. 5*A*). PJ-34 appeared to be less potent than BYK on *Notch3* at both mRNA and protein levels in our experimental setting (Fig. 5*A*) and in others (41). Thus, we used BYK to test the effect on *HEY1* and *HES1* expression under hypoxia. Compared to the effect on *Notch3* expression (Fig. 5*A*), BYK effects on *HEY1* and *HES1* were weak or null (Fig. S4). This is possibly because these genes are not efficient targets of *Notch3* in this cell line or longer BYK treatment is required for efficient suppression of the downstream targets, in addition to the unexpected nonspecific enhancement of the basal levels in normoxia. These data indicated that the hypoxic induction of *Notch3* was highly dependent on PARP-1 and that more supporting data might be required to reveal the regulation of the Notch3 downstream genes (*HEY1* and *HES1*) under hypoxia. At the protein level, PARP inhibitors reduced N3ICD under hypoxia without affecting PARP-1 levels *per se*. Interestingly, PARP inhibitors did not affect the protein levels of PARP-1 but clearly decreased HIF-1α under hypoxia (Fig. 5*B*), which is consistent with the previous observation with PJ-34, olaparib, or PARP-1 inhibitor (DPQ) (39, 42). Somewhat conflictingly, HIF-1α protein levels were not suppressed by siPARP-1s (Fig. S3*B*). More efficient suppression or a longer duration time than 24 h could be required to exert effects of siPARP-1s, which is an issue in future studies. Inhibition of PARP activity might affect the protein stability of HIF-1α during hypoxia. The effect of siPARP-1 or PARP inhibitor treatment on HIF-1α alone has a limited effect on the expression of *PGK1* and *CA9* (HRE-dependent HIF-1α downstream targets). On the other hand, dual inhibition of PARP and HIF-1α actions by PARP inhibitors potentiates suppression of Notch3 under hypoxia.

Discussion

In this study, we show that (1) *Notch3* expression is increased at mRNA and protein levels under hypoxia dependent on HIF-1α, (2) the *Notch3* promoter activity is induced by hypoxia or HIF-1α and HIF-1α binds to and activates the *Notch3* promoter that lacks the HRE sequence, (3) PARP-1 binds to the *Notch3* promoter and is required for activation, and (4) PARP inhibitors as well as siRNA targeting PARP-1 downregulate *Notch3* expression. High expression of *Notch3* is observed in various types of cancer and is correlated with poor overall survival, distant metastasis, and chemoresistance (43). In prostate cancer, mRNA and protein levels of *Notch3* are induced by hypoxia, and high-intensity HIF-1α and VEGF immunostaining biopsy samples showed high Notch3 expression (14). Analysis of the knockout mouse of prolyl hydroxylase domain protein-2, which is a well-known negative regulator of HIF-1α protein, indicated that mRNA and protein levels of *Notch3* are significantly upregulated in prolyl hydroxylase domain protein-2 KO endothelial cells (44). Overexpression of HIF-1α in liver cancer cell lines increases both

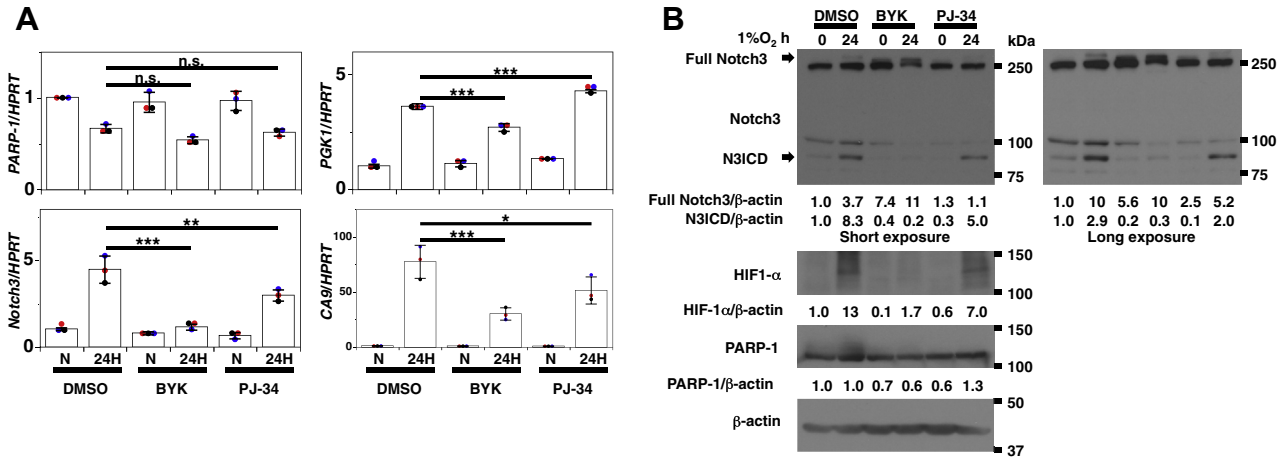

Figure 5. PARP inhibitors, especially PARP-1-specific inhibitor, attenuate induction of Notch3 by hypoxia. *A* and *B*, SK-N-BE(2)c cells were treated with DMSO or PARP inhibitor (BYK204165 or PJ-34) and incubated under normoxia or hypoxia for 24 h. *A*, expression levels of *PARP-1*, *Notch3*, *PGK1*, and *CA9* were analyzed by RT-qPCR. Relative mRNA levels were calculated as the ratio to that of *HPRT*. The statistical analysis was performed and shown in the same way as Figure 1*A*. *$p < 0.05$; **$p < 0.01$; ***$p < 0.001$. *B*, protein levels of Notch3, HIF-1α, PARP-1, and β-actin were evaluated by immunoblotting. *Arrows* indicate Full Notch3 and N3ICD bands. Values by quantification after normalized to DMSO in 1% O_2 for 0 h are presented under the lanes. HIF-1α, hypoxia-inducible factor-1α; Full Notch3, full-length Notch3; N3ICD, Notch3 intracellular domain; n.s., not significant; PARP, poly [ADP-ribose] polymerase; RT-qPCR, reverse transcription-quantitative PCR.

mRNA and protein levels of *Notch3*, and increased Notch3 levels are closely correlated with vascular invasiveness in liver cancer tissues (45). *Notch3* promoter activity was induced by hypoxia or HIF-1α, and HIF-1α could bind to the *Notch3* promoter without canonical binding elements. Our pull-down assays demonstrated that HIF-1α binding to the *Notch3* promoter sequence is dependent on PARP-1. We next referred to the ChIP-Atlas (https://chip-atlas.org/) (46) for further information. Supporting our findings, the database shows that HIF-1α binds to the *Notch3* promoter region with no HRE sequence (Fig. S5). Interestingly, the C-terminal but not the N-terminal region of HIF-1α was required for the activation of *Notch3*, which could also mean that HIF-1α does not directly bind to the DNA sequence and another protein is involved in HIF-1α binding. There are several reports that HIF-1α interacts with other DNA binding factors and regulates target gene expression. For stem cell maintenance, HIF-1α binds to Notch1 ICD and the complexes bind to the Notch responsive promoters to activate Notch downstream genes (*Hey* and *Hes*) (23). In tumor cells under hypoxia, complexes of HIF-1α and Notch1 ICD bind to the promoter of *Snail-1*, which is a Notch target gene, and elevate the expression to increase cell invasion (24). In addition, GABP interacts with HIF-1α and binds to the *Hes1* promoter to respond to hypoxia in P19 cells (25).

To identify DNA-binding factors that bind to the *Notch3* promoter with HIF-1α, we performed pull-down and mass spectrometry analyses. The results revealed that PARP-1 could bind to the *Notch3* promoter region, and we analyzed the functional effect of PARP-1 on *Notch3* promoter activity. The results of the cotransfection assay using the *Notch3* promoter reporter and PARP-1 expression plasmid showed that the full-length PARP-1 actually activated *Notch3* reporter activity and, in addition, acted on −57 to −10 bp upstream of *Notch3* transcription start site.

ChIP analyses have shown that PARP-1 is preferentially detected in the active transcription promoter locus (47, 48). It is also noteworthy that *Notch3* expression is significantly decreased in the *Parp-1* $^{-/-}$ embryonic stem cells (35). The *Notch3* promoter sequence proximal to the transcription start site is extremely guanine-rich, which is highly conserved across mammals (Fig. S6). This stretch can form G-quadruplex (G4) structures. Interestingly, it was reported that PARP-1 binds to the G4 motif of *c-Myc* and *KRAS* promoters and activates their transcription (49, 50). It is tempting to speculate that PARP-1 activates *Notch3* transcription by interacting with the G4 motifs present in the *Notch3* promoter. Further analyses are needed to confirm this hypothesis.

There are limitations to this study and further work remains to be done. We did not make an attempt to detect the colocalization of endogenous HIF-1α and PARP-1 on the *Notch3* promoter and the correlation to *Notch3* expression. As a future study, we will perform ChIP analyses with or without treatment with hypoxia or a PARP inhibitor.

In conclusion, we have demonstrated that HIF-1α and PARP-1 cooperatively and transcriptionally regulate *Notch3* expression during hypoxia. The mechanisms we suggest here are as follows: HIF-1α stabilized by hypoxia makes complexes with PARP-1; thereafter, PARP-1 binds to a guanine-rich region, possibly a G4 motif, in the *Notch3* promoter, and, finally, HIF-1α tethered on PARP-1 activates *Notch3* transcription by employing the HIF-1α–activating domain. (Fig. 6). Since inhibition of PARP was effective in suppressing Notch3 under hypoxia, enzymatic activities of PARP appear to be also important in the mechanism. In this context, our findings may contribute to a diagnostic strategy (*i.e.*, utilization of HIF-1α and Notch3 expression as an index) for the treatment with PARP inhibitors. A large number of reports have shown that PARP-1 plays a critical role in gene expression; however, its molecular mechanisms have not been elucidated. Our results may provide a clue to understanding the novel aspects of PARP-1 molecular function as well as the critical involvement of hypoxia and HIF-1α in oncogenesis driven by Notch3.

Experimental procedures

Cell culture and hypoxia treatment

Human neuroblastoma SK-N-BE(2)c and SK-N-FI cell lines were maintained in RPMI 1620 supplemented with 10% fetal bovine serum, 50 IU/ml penicillin, and 50 mg/ml streptomycin sulfate. HeLa cells were grown in Dulbecco's modified Eagle's medium supplemented with 10% fetal bovine serum, 50 IU/ml penicillin, and 50 mg/ml streptomycin sulfate. All media, growth factors, and antibiotics were purchased from Invitrogen. All cells were routinely screened for *Mycoplasma* using a MycoAlert detection kit (Lonza). For the incubation of cells under hypoxia, cells were placed in a hypoxia workstation, Invivo O_2 400 (Ruskinn) at 1% oxygen. To analyze PARP function, 15 μM of BYK204165 (Sigma-Aldrich) or PJ-34 (Sigma-Aldrich) was added to the growth medium.

RNA preparation and RT-qPCR

Total RNA was prepared using the NucleoSpin RNA II kit (MACHEREY-NAGEL), and complementary DNA was synthesized from 1 μg of the total RNA extracted from cell lines using the cDNA synthesis kit (Thermo Fisher Scientific), according to the manufacturer's instructions. Quantitative PCR was performed on the ABI 7300 sequence detector and

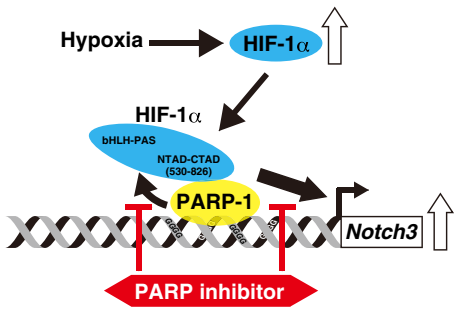

Figure 6. Hypothetical model for Notch3 regulation by cooperative actions of HIF-1α and PARP-1. HIF-1α stabilized under hypoxia forms a complex with PARP-1 bound to the *Notch3* promoter comprising guanine-rich stretches. This complex subsequently activates *Notch3* transcription by employing the HIF-1α C-terminal activating domain. PARP inhibitor attenuates the activation of *Notch3 via* suppressing the catalytic activity of PARP-1 to HIF-1α. HIF-1α, hypoxia-inducible factor-1α; PARP, poly [ADP-ribose] polymerase.

QuantStudio3 (Applied Biosystems) using Power SYBR Green PCR Master Mix (Applied Biosystems). Primers are listed in Table S1. The expression level of *HPRT* was measured for normalization of the RT-qPCR data. Relative expression levels were calculated using the comparative Ct method. All experiments were performed in triplicate and repeated three times.

RNA interference

siRNAs against *HIF-1A*, *PARP-1*, and negative control siRNA (siNS) (Table S2) were purchased from Qiagen or Ambion. Cells were seeded in a 6-cm dish, 24 h before siRNA transfection. Transient siRNA transfection was performed using Lipofectamine 2000 (Invitrogen), according to the manufacturer's instructions. Thereafter, the cells were cultured for 24 h under normoxia or hypoxia before harvest. The harvested cells were analyzed using RT-qPCR or immunoblotting.

Immunoblotting

For protein expression analysis, whole-cell extracts were prepared from cultured cells as previously described (51). Aliquots of 25 or 50 μg of extract were separated by SDS-PAGE and blotted onto PVDF membranes. Anti-Notch3, anti–PARP-1 (CST), anti–HIF-1α (BD Biosciences Pharmingen and GeneTex), anti-FLAG (Sigma-Aldrich), and anti–β-actin (Sigma-Aldrich) were used as primary antibodies. Mouse or rabbit anti-IgG horseradish peroxidase conjugate (Amersham Biosciences) was used as the secondary antibodies. Immunocomplexes were visualized using enhanced chemiluminescence reagent ECL Plus (Amersham Biosciences). Specific bands were quantified by measuring densities using Image Studio Lite v. 5.2.5 software (https://www.licor.com/bio/image-studio-lite/).

Plasmid constructions

A 265-bp DNA fragment (nucleotide positions from −188 to +77 assuming the transcriptional start site is +1; GenBank: NM_000435.3), including the promoter region of *Notch3*, was amplified by PCR from a HepG2 genomic DNA and subcloned into the luciferase reporter plasmid pGL4.10 as described before (52). The reporter was designated as pGL4.10 *Notch3* pro −188 bp. A series of 5′ deletion mutants of pGL4.10 *Notch3* pro were constructed by PCR using internal specific primer sets with pGL4.10 *Notch3* pro −188 bp as a template. Details of the expression plasmid vector of p3XFLAG HIF-1α 2-826 have been previously described (53). A series of HIF-1α deletion mutants were constructed by PCR using internal specific primers and site-direct mutagenesis primer sets with p3XFLAG HIF-1α 2-826 as a template. p3XFLAG PARP-1 2-1014 was constructed by inserting the PARP-1 cDNA fragment of pQC FLAG PARP-1 IH (kindly provided by Dr Sekine) into p3XFLAG. p3XFLAG PARP-1 2-533 and 531-1014 were generated by PCR site-directed mutagenesis using p3XFLAG PARP-1 2-1014 as a template. All constructs were confirmed by sequence analysis.

Luciferase reporter assay

HeLa cells were seeded in 24-well plates and cultured for 24 h before transient transfection. Transient transfection was performed as follows: pGL4.10 *Notch3* pro (100–200 ng) with or without p3XFLAG, p3XFLAG HIF-1α, or p3XFLAG PARP-1 (100 ng) were mixed with Lipofectamine 2000 transfection reagent (Invitrogen). Cells were grown under normoxia or hypoxia for 24 h after transfection, and then analysis of luciferase reporter activity was performed. After growth, the cells were lysed using cell culture lysis buffer (Promega), according to the manufacturer's instructions. Total cell lysates were used to measure luciferase activity using GloMax (Promega) with a Luciferase assay kit (Bio-Thema). Protein concentrations of lysates were determined to normalize luciferase activities by the Bradford method (Bio-Rad). All experiments were performed three times each with triplicate.

Biotin-streptavidin pull-down assay

Single-stranded *Notch3* promoter sense oligonucleotide 5′-biotin-TEG GGCCCCGGGGCGGGGCGAGCCTTCGAGGGCTGGGGGCGGGGCGGCCCGG-3′ and antisense oligonucleotide 5′-CCGGGCCGCCCCGCCCCCAGCCCTCGAAGGCTCGCCCCGCCCCGGGGCC-3′ (Thermo Fisher Scientific) were annealed by heating at 95 °C for 5 min and cooling down slowly to room temperature. One milligram of nuclear extracts from HeLa cells cultured under normoxia or hypoxia was incubated overnight at 4 °C with the annealed oligonucleotides bound to streptavidin agarose in the presence of poly dI-dC as a nonspecific competitor. The oligonucleotide and streptavidin bead complexes were washed four times with washing buffer. SDS-sample buffer was added to the samples, and the mixtures were incubated at 95 °C for 5 min. Proteins were analyzed by immunoblotting or stained using the SilverQuest Silver Staining Kit (Invitrogen). Single-stranded *Notch3* promoter sense oligonucleotides without biotin-TEG and antisense oligonucleotides were hybridized using the method previously described in this article. In this experiment, a double-stranded control oligonucleotide with a sense oligonucleotide 5′-TAAAAGCTGTCTCAGCCCTAAAAGCTGTCTCAGCCCTAAAAGCTGTCTC-3′ and antisense oligonucleotide 5′-GAGACAGCTTTTAGGGCTGAGACAGCTTTTAGGGCTGAGACAGCTTTTA-3′ (Thermo Fisher Scientific) was used, as this has been used as an HRE-less control (25).

Mass spectrometry analysis

Pull-down protein complexes using biotinylated oligo and streptavidin agarose were resolved on a 10% SDS-PAGE gel (Bio-Rad). Protein bands were stained with SimplyBlue SafeStain (Thermo Fisher Scientific) and excised. Protein identification was carried out by ProtTech, Inc. The analytical setting of mass spectrometry is described in the supporting methods. The detailed results and peptide sequences of mass spectrometry analysis are presented in Tables S3 and S4.

Pull-down assay for protein–protein interaction

N-terminally F-HIF-1α on a lentivirus vector (54) was stably expressed in HeLa and used for pull-down assay with M2 agarose (Sigma-Aldrich). Nuclear extracts were prepared by isolating nuclei with hypotonic buffer (20 mM Tris–HCl (pH 7.9), 10 mM KCl, 1 mM $MgCl_2$, 0.2 mM EDTA, 0.5 mM DTT, 10% glycerol, 0.5% NP40, and 0.5 mM PMSF) and then extracting with buffer D (54), containing 400 mM NaCl, cOmplete (Sigma-Aldrich) and 0.5 mM PMSF. The final salt concentration of nuclear extracts was adjusted to 200 mM NaCl with buffer D upon pull-down assay. Washing and elution conditions were previously described (54).

Pull-down assay for PARP-1–dependent HIF-1α binding to the Notch3 promoter sequence

PARP-1, the full-length HIF-1α or a C-terminal region (530–826) of HIF-1α, all FLAG-tagged, was transiently overexpressed in 293T cells and purified using M2 agarose (Sigma-Aldrich) and a FLAG peptide for elution. Biotin-labeled *Notch3* promoter sequence oligo bound on streptavidin-sepharose was incubated with HIF-1α in the presence or absence of PARP-1. After washing with buffer D containing 150 mM NaCl, bound protein fractions were subjected to immunoblotting.

Statistical analysis

All luciferase and RT-qPCR analyses were performed three times (three biological replicates) each with three technical samples. The individual mean values calculated from the three technical samples were shown in different color dot plots (black, red, and blue). The overall mean values and SD were then calculated and presented as a bar graph and an error bar. Statistical significance of the difference between group means was performed by one-way ANOVA test, and a post hoc test was carried out using Dunnett's test or Tukey-Kramer HSD test. All statistical tests were performed using JMP version 5.0 software (https://www.jmp.com/en_in/home.html).

Data availability

All data relevant to these studies are present in the article and the supporting information.

Supporting information—This article contains supporting information.

Acknowledgments—We thank Dr Yoshiaki Fujii-Kuriyama and all LP lab members for their technical assistance and helpful comments on this work. We also thank all members of the Karolinska Institutet (KI) and Cancer Science Institute of Singapore (CSI Singapore) for their technical and secretarial support. Scientific interactions between KI and CSI Singapore were conducted under CSI Singapore grants, and among them, H. N's visit to CSI Singapore was the driving force for developing this project. RT-qPCR was performed at the Analytical Research Center for Experimental Sciences, Saga University. H. K. appreciates generous coverage by CSI Singapore. Prof. Lorenz Poellinger (55, 56) passed away during the reporting phase of this study; therefore, we have dedicated this work to his memory.

Author contributions—H. N., H. K., and L. P. conceptualization; H. N. validation; H. N. formal analysis; H. N., H. S., H. K., and K. G. investigation; H. N., H. S., H. K., K. G., and L. P. writing–original draft; H. N., H. S., H. K., H. M., K. G., and L. P. writing–review and editing; H. N., H. M., and L. P. funding acquisition; H. S. and K. G. resources; L. P. supervision; H. N., H. K., and L. P. methodology.

Funding and additional information—This work was supported by grants from the Singapore National Research Foundation (R-713-005-014-271 and R-713-000-162-511) and the Singapore Ministry of Education under its Research Centres of Excellence initiatives, the Singapore Ministry of Health's National Medical Research Council under its Clinician Scientist Individual Research Grant (NMRC/CIRG/1389/2014), the Swedish Research Council, the Swedish Cancer Society, and the Swedish Childhood Cancer Foundation to L. P. and from the Japanese Society for the Promotion of Science, KAKENHI (20K07700 and 20H00463) to H. N. and H. M., respectively. H. N. acknowledges the Wenner-Gren Foundation for fellowship support from 2009 to 2011, when part of this research was performed at Karolinska Institutet.

Conflict and interest—The authors declare that they have no conflicts of interest with the contents of this article.

Abbreviations—The abbreviations used are: F-HIF-1α, FLAG-tagged HIF-1α; G4, G-quadruplex; HIF, hypoxia-inducible factor; HRE, hypoxia response element; N3ICD, Notch3 intracellular domain; PARP, poly [ADP-ribose] polymerase; RT-qPCR, reverse transcription-quantitative PCR; siNS, nonspecific siRNA; siPARP-1s, siRNAs targeting RARP-1.

References

1. Siebel, C., and Lendahl, U. (2017) Notch signaling in development, tissue homeostasis, and disease. *Physiol. Rev.* **97**, 1235–1294
2. Andersson, E. R., Sandberg, R., and Lendahl, U. (2011) Notch signaling: Simplicity in design, versatility in function. *Development* **138**, 3593–3612
3. Aburjania, Z., Jang, S., Whitt, J., Jaskula-Stzul, R., Chen, H., and Rose, J. B. (2018) The role of Notch3 in cancer. *Oncologist* **23**, 900–911
4. Hosseini-Alghaderi, S., and Baron, M. (2020) Notch3 in development, health and disease. *Biomolecules* **10**, 485
5. Xiong, J., Zhang, X., Chen, X., Wei, Y., Lu, D. G., Han, Y. W., *et al.* (2017) Prognostic roles of mRNA expression of notch receptors in non-small cell lung cancer. *Oncotarget* **8**, 13157–13165
6. Wu, X., Liu, W., Tang, D., Xiao, H., Wu, Z., Chen, C., *et al.* (2016) Prognostic values of four Notch receptor mRNA expression in gastric cancer. *Sci. Rep.* **6**, 28044
7. Landor, S. K. J., Santio, N. M., Eccleshall, W. B., Paramonov, V. M., Gagliani, E. K., Hall, D., *et al.* (2021) PIM-induced phosphorylation of Notch3 promotes breast cancer tumorigenicity in a CSL-independent fashion. *J. Biol. Chem.* **296**, 100593
8. Kang, W., Zhang, J., Huang, T., Zhou, Y., Wong, C. C., Chan, R. C. K., *et al.* (2021) NOTCH3, a crucial target of miR-491-5p/miR-875-5p, promotes gastric carcinogenesis by upregulating PHLDB2 expression and activating Akt pathway. *Oncogene* **40**, 1578–1594
9. Shi, C., Qian, J., Ma, M., Zhang, Y., and Han, B. (2014) Notch 3 protein, not its gene Polymorphism, is associated with the chemotherapy response and prognosis of advanced NSCLC Patients. *Cell Physiol. Biochem.* **34**, 743–752

10. Konishi, J., Kawaguchi, K. S., Vo, H., Haruki, N., Gonzalez, A., Carbone, D. P., *et al.* (2007) Gamma-secretase inhibitor prevents Notch3 activation and reduces proliferation in human lung cancers. *Cancer Res.* **67**, 8051–8057
11. Goruganthu, M. U. L., Shanker, A., Dikov, M. M., and Carbone, D. P. (2020) Specific targeting of notch ligand-receptor interactions to modulate immune responses: a Review of clinical and preclinical findings. *Front. Immunol.* **11**, 1958
12. Yen, W. C., Fischer, M. M., Axelrod, F., Bond, C., Cain, J., Cancilla, B., *et al.* (2015) Targeting Notch signaling with a Notch2/Notch3 antagonist (tarextumab) inhibits tumor growth and decreases tumor-initiating cell frequency. *Clin. Cancer Res.* **21**, 2084–2095
13. Danza, G., Di Serio, C., Ambrosio, M. R., Sturli, N., Lonetto, G., Rosati, F., *et al.* (2013) Notch3 is activated by chronic hypoxia and contributes to the progression of human prostate cancer. *Int. J. Cancer* **133**, 2577–2586
14. Meunier, A., Flores, A. N., McDermott, N., Rivera-Figueroa, K., Perry, A., Lynch, T., *et al.* (2016) Hypoxia regulates Notch-3 mRNA and receptor activation in prostate cancer cells. *Heliyon* **2**, e00104
15. Yao, J., Fang, X., Zhang, C., Yang, Y., Wang, D., Chen, Q., *et al.* (2021) Astragaloside IV attenuates hypoxia-induced pulmonary vascular remodeling *via* the Notch signaling pathway. *Mol. Med. Rep.* **23**, 1
16. Harris, A. L. (2002) Hypoxia–a key regulatory factor in tumour growth. *Nat. Rev. Cancer* **2**, 38–47
17. Vaupel, P., and Mayer, A. (2007) Hypoxia in cancer: significance and impact on clinical outcome. *Cancer Metastasis Rev.* **26**, 225–239
18. Rankin, E. B., and Giaccia, A. J. (2016) Hypoxic control of metastasis. *Science* **352**, 175–180
19. Semenza, G. L. (2010) Defining the role of hypoxia-inducible factor 1 in cancer biology and therapeutics. *Oncogene* **29**, 625–634
20. Dengler, V. L., Galbraith, M., and Espinosa, J. M. (2014) Transcriptional regulation by hypoxia inducible factors. *Crit. Rev. Biochem. Mol. Biol.* **49**, 1–15
21. Rankin, E. B., and Giaccia, A. J. (2008) The role of hypoxia-inducible factors in tumorigenesis. *Cell Death Differ* **15**, 678–685
22. Simon, M. C. (2016) The hypoxia response pathways - hats off. *N. Engl. J. Med.* **375**, 1687–1689
23. Gustafsson, M. V., Zheng, X., Pereira, T., Gradin, K., Jin, S., Lundkvist, J., *et al.* (2005) Hypoxia requires notch signaling to maintain the undifferentiated cell state. *Dev. Cell* **9**, 617–628
24. Sahlgren, C., Gustafsson, M. V., Jin, S., Poellinger, L., and Lendahl, U. (2008) Notch signaling mediates hypoxia-induced tumor cell migration and invasion. *Proc. Natl. Acad. Sci. USA* **105**, 6392–6397
25. Zheng, X., Narayanan, S., Zheng, X., Luecke-Johansson, S., Gradin, K., Catrina, S. B., *et al.* (2017) A Notch-independent mechanism contributes to the induction of Hes1 gene expression in response to hypoxia in P19 cells. *Exp. Cell Res.* **358**, 129–139
26. Barkauskaite, E., Jankevicius, G., and Ahel, I. (2015) Structures and mechanisms of enzymes employed in the synthesis and degradation of PARP-dependent protein ADP-ribosylation. *Mol. Cell* **58**, 935–946
27. Abbotts, R., and Wilson, D. M., 3rd. (2017) Coordination of DNA single strand break repair. *Free Radic. Biol. Med.* **107**, 228–244
28. Hou, W. H., Chen, S. H., and Yu, X. (2019) Poly-ADP ribosylation in DNA damage response and cancer therapy. *Mutat. Res.* **780**, 82–91
29. O'Connor, M. J. (2015) Targeting the DNA damage response in cancer. *Mol. Cell* **60**, 547–560
30. Mateo, J., Lord, C. J., Serra, V., Tutt, A., Balmana, J., Castroviejo-Bermejo, M., *et al.* (2019) A decade of clinical development of PARP inhibitors in perspective. *Ann. Oncol.* **30**, 1437–1447
31. Schiewer, M. J., and Knudsen, K. E. (2014) Transcriptional roles of PARP1 in cancer. *Mol. Cancer Res.* **12**, 1069–1080
32. Weaver, A. N., and Yang, E. S. (2013) Beyond DNA repair: additional functions of PARP-1 in cancer. *Front. Oncol.* **3**, 290
33. Ray Chaudhuri, A., and Nussenzweig, A. (2017) The multifaceted roles of PARP1 in DNA repair and chromatin remodelling. *Nat. Rev. Mol. Cell Biol.* **18**, 610–621
34. Ko, H. L., and Ren, E. C. (2012) Functional aspects of PARP1 in DNA repair and transcription. *Biomolecules* **2**, 524–548
35. Ogino, H., Nozaki, T., Gunji, A., Maeda, M., Suzuki, H., Ohta, T., *et al.* (2007) Loss of Parp-1 affects gene expression profile in a genome-wide manner in ES cells and liver cells. *BMC Genomics* **8**, 41
36. Nirodi, C., NagDas, S., Gygi, S. P., Olson, G., Aebersold, R., and Richmond, A. (2001) A role for poly(ADP-ribose) polymerase in the transcriptional regulation of the melanoma growth stimulatory activity (CXCL1) gene expression. *J. Biol. Chem.* **276**, 9366–9374
37. Simbulan-Rosenthal, C. M., Rosenthal, D. S., Luo, R., Samara, R., Espinoza, L. A., Hassa, P. O., *et al.* (2003) PARP-1 binds E2F-1 independently of its DNA binding and catalytic domains, and acts as a novel coactivator of E2F-1-mediated transcription during re-entry of quiescent cells into S phase. *Oncogene* **22**, 8460–8471
38. Elser, M., Borsig, L., Hassa, P. O., Erener, S., Messner, S., Valovka, T., *et al.* (2008) Poly(ADP-ribose) polymerase 1 promotes tumor cell survival by coactivating hypoxia-inducible factor-1-dependent gene expression. *Mol. Cancer Res.* **6**, 282–290
39. Marti, J. M., Garcia-Diaz, A., Delgado-Bellido, D., O'Valle, F., Gonzalez-Flores, A., Carlevaris, O., *et al.* (2021) Selective modulation by PARP-1 of HIF-1alpha-recruitment to chromatin during hypoxia is required for tumor adaptation to hypoxic conditions. *Redox Biol.* **41**, 101885
40. Hulse, M., Caruso, L. B., Madzo, J., Tan, Y., Johnson, S., and Tempera, I. (2018) Poly(ADP-ribose) polymerase 1 is necessary for coactivating hypoxia-inducible factor-1-dependent gene expression by Epstein-Barr virus latent membrane protein 1. *PLoS Pathol.* **14**, e1007394
41. Luo, X., Ryu, K. W., Kim, D. S., Nandu, T., Medina, C. J., Gupte, R., *et al.* (2017) PARP-1 controls the adipogenic transcriptional Program by PARylating C/EBPbeta and modulating its transcriptional activity. *Mol. Cell* **65**, 260–271
42. Martin-Oliva, D., Aguilar-Quesada, R., O'Valle, F., Munoz-Gamez, J. A., Martinez-Romero, R., Garcia Del Moral, R., *et al.* (2006) Inhibition of poly(ADP-ribose) polymerase modulates tumor-related gene expression, including hypoxia-inducible factor-1 activation, during skin carcinogenesis. *Cancer Res.* **66**, 5744–5756
43. Xiu, M., Wang, Y., Li, B., Wang, X., Xiao, F., Chen, S., *et al.* (2021) The role of Notch3 signaling in cancer stemness and chemoresistance: molecular mechanisms and targeting strategies. *Front. Mol. Biosci.* **8**, 694141
44. Wang, S., Zeng, H., Chen, S. T., Zhou, L., Xie, X. J., He, X., *et al.* (2017) Ablation of endothelial prolyl hydroxylase domain protein-2 promotes renal vascular remodelling and fibrosis in mice. *J. Cell Mol. Med.* **21**, 1967–1978
45. Yang, S. L., Ren, Q. G., Zhang, T., Pan, X., Wen, L., Hu, J. L., *et al.* (2017) Hepatitis B virus X protein and hypoxia-inducible factor-1alpha stimulate Notch gene expression in liver cancer cells. *Oncol. Rep.* **37**, 348–356
46. Oki, S., Ohta, T., Shioi, G., Hatanaka, H., Ogasawara, O., Okuda, Y., *et al.* (2018) ChIP-atlas: a data-mining suite powered by full integration of public ChIP-seq data. *EMBO Rep.* **19**, e46255
47. Krishnakumar, R., Gamble, M. J., Frizzell, K. M., Berrocal, J. G., Kininis, M., and Kraus, W. L. (2008) Reciprocal binding of PARP-1 and histone H1 at promoters specifies transcriptional outcomes. *Science* **319**, 819–821
48. Nalabothula, N., Al-jumaily, T., Eteleeb, A. M., Flight, R. M., Xiaorong, S., Moseley, H., *et al.* (2015) Genome-Wide Profiling of PARP1 reveals an interplay with gene regulatory regions and DNA methylation. *PLoS One* **10**, e0135410
49. Prigent, C., Fekete, A., Kenesi, E., Hunyadi-Gulyas, E., Durgo, H., Berko, B., *et al.* (2012) The guanine-quadruplex structure in the human c-myc Gene's promoter is converted into B-DNA form by the human poly(ADP-Ribose)Polymerase-1. *PLoS One* **7**, e42690
50. Cogoi, S., Paramasivam, M., Membrino, A., Yokoyama, K. K., and Xodo, L. E. (2010) The KRAS promoter responds to Myc-associated zinc finger and poly(ADP-ribose) polymerase 1 proteins, which recognize a critical quadruplex-forming GA-element. *J. Biol. Chem.* **285**, 22003–22016

51. Nakamura, H., Tanimoto, K., Hiyama, K., Yunokawa, M., Kawamoto, T., Kato, Y., *et al.* (2008) Human mismatch repair gene, MLH1, is transcriptionally repressed by the hypoxia-inducible transcription factors, DEC1 and DEC2. *Oncogene* **27**, 4200–4209
52. Nakamura, H., Bono, H., Hiyama, K., Kawamoto, T., Kato, Y., Nakanishi, T., *et al.* (2018) Differentiated embryo chondrocyte plays a crucial role in DNA damage response *via* transcriptional regulation under hypoxic conditions. *PLoS One* **13**, e0192136
53. Khalesi, E., Nakamura, H., Lee, K. L., Putra, A. C., Fukazawa, T., Kawahara, Y., *et al.* (2013) The Krüppel-like zinc finger transcription factor, GLI-similar 1, is regulated by hypoxia-inducible factors *via* non-canonical mechanisms. *Biochem. Biophys. Res. Commun.* **441**, 499–506
54. Sun, W., Kato, H., Kitajima, S., Lee, K. L., Gradin, K., Okamoto, T., *et al.* (2017) Interaction between von Hippel-lindau protein and fatty acid synthase modulates hypoxia target gene expression. *Sci. Rep.* **7**, 7190
55. Lendahl, U. (2017) Lorenz Poellinger MD, PhD (1957-2016). *Cell Death Differ.* **24**, 571
56. Giaccia, A., and Johnson, R. S. (2017) Lorenz Poellinger. *Exp. Cell Res.* **356**, 115